A Universal High-Resolution Micro-Patterning Technique for Solution-Processed Materials

John Leo Velpugonda

A thesis
submitted in partial fulfillment of the
requirements for the degree of

Master of Science

University of Washington

2024

Committee:

Lih Y Lin

M P Anantram

Program Authorized to Offer Degree:
Electrical and Computer Engineering

University of Washington

Abstract

A Universal High-Resolution Micro-Patterning Technique for Solution-Processed Materials

John Leo Velpugonda

Chair of the Supervisory Committee:
Prof. Lih Y Lin
Department of Electrical and Computer Engineering

A universal method of micro-patterning thin quantum dot films is highly desired by industry to enable integration of quantum dot(QD) materials with optoelectronic devices. Many of the methods reported so far, including specially engineered photoresist or ink-jet printing, are either of poor yield, resolution limited, difficult to scale for mass production, overly expensive or sacrifice some optical quality of the quantum dots. Dry photolithographic lift-off method is a promising solution for pixelization of solution-processed materials. Recent work demonstrated patterning of perovskite quantum dot pixels, 10 µm in diameter, to construct a static micro-display. This thesis presents an advancement of this method demonstrating high-resolution patterning (1 µm diameter) with full-scale processing on 100 mm wafer, and multi-color integration of two different varieties of quantum dots.

In this work, both perovskite and cadmium-selenide quantum dots were employed, though the method is adaptable to other solution-processed materials. Specifically, green perovskite quantum dots were synthesized using a room-temperature ligand-assisted reprecipitation method, resulting in a photoluminescent quantum yield of 93.6% and a full-width half-maximum emission linewidth of less than 20 nm. The thesis also explores the synthesis and characterization of these QDs.

These results demonstrate the viability of this method for use in scalable manufacturing of high-resolution micro-displays. Future work will focus on integrating UV or blue pixel sources with multi-color patterning to realize a full-color display, further pushing the

boundaries of this promising technology.

TABLE OF CONTENTS

LIST OF FIGURES

ACKNOWLEDGMENTS

I would like to express my deepest gratitude to my friends and family who have supported me throughout this journey. Thank you, Mom and Dad, for your unwavering support and for always encouraging me to move in the right direction. I am deeply grateful for having such loving and supportive parents.

I extend my sincere thanks to my supervisor, Prof. Lih Lin, without whom I would not have been able to complete my master's program. Your inspiration and guidance have been instrumental, especially as I transitioned into a new field. Moving from my undergraduate discipline has been challenging at times, but your kind words and mentorship have made a significant difference. I am excited to continue my academic journey with you as my PhD supervisor. I would like to thank Prof. M P Anantram for being a part of my thesis committee and also for the wonderful and inspiring lectures on Quantum Mechanics. Your teachings have greatly enriched my understanding and appreciation of the subject.

I would also like to thank my group members, Rose Johnson and Ethan Keeler. Working with you at the WNF, PRC, and RTT has been an invaluable learning experience. Additionally, I am grateful to Matthew Yerich and Naresh Varnakavi for your valuable insights about research.

Finally, I would like to thank University of Washington for providing the facilities for my research. I would like to acknowledge the funding resources for my research. This work is supported by the National Science Foundation (Award No. IIP-2140788), the University of Washington CoMotion Innovation Gap Fund, and the Washington Research Foundation. Part of material synthesis and characterization was supported by the National Science Foundation through Award No. CMMI-2227285 and the Science and Technology Center (STC) for Integration of Modern Optoelectronic Materials on Demand (IMOD) under Award No. DMR-2019444. Part of device fabrication was conducted at the Washington

Nanofabrication Facility, a National Nanotechnology Coordinated Infrastructure (NNCI) site at the University of Washington supported by the National Science Foundation (NSF) (grant NNCI-1542101). The AFM and TEM imaging were performed at the UW Molecular Analysis Facility, part of the NSF NNCI to coordinate nanoscale research and development activities across the United States and is supported by NNCI-2025489 and NNCI-1542101.

Chapter 1

INTRODUCTION AND MOTIVATION

Micro-light-emitting diode (micro-LED) display technology holds significant promise for a wide range of consumer and commercial applications, such as augmented and virtual reality headsets, smartwatches, and next-generation mobile devices. These displays offer many advantages over traditional display technologies like LCD and OLED, boasting higher brightness, improved contrast, and very small pixel size, making them an attractive choice for compact, high-resolution displays [1, 2]. The term micro-LED typically refers to LEDs with dimensions smaller than 100 μm [3]. And a significant challenge in developing micro-LED displays is the miniaturization of individual LED elements.

The dominant technology for assembling a full-color LED display, known as pick-and-place, involves integrating LEDs from three separate substrates, each optimized for a specific color wavelength. This approach allows for the precise engineering of the active regions to achieve optimal performance for red, green, and blue emitters. However, transferring and assembling these microscopic LED chips onto a display backplane is intricate and resource-intensive, posing limitations on the resulting displays' achievable resolution, yield, and cost-effectiveness[4]. Fluidic self-assembly has been explored to circumvent this manufacturing challenge, and recent work demonstrated self-assembly of more than 19,000 gallium-nitride (GaN) chiplets 45 μm in diameter, in a research setting [5].

An alternative, widely used approach for display colorization, which avoids the technical challenges of mass transfer methods, is the integration of a photoluminescent color converting film onto blue LEDs [6]. This approach takes advantage of the superior luminous efficiency and manufacturing maturity of blue GaN LEDs. Every display pixel comprises three blue sub-pixels, two of them encapsulated by a red or green color-converting layer. Rare-earth phosphors are widely used for photoluminescent color conversion; their large particle size inhibits their uniform coating on micro-LEDs [7]. Quantum dots (QDs) have

garnered significant attention as a color-conversion material due to their exceptional optical properties, including narrow emission line widths, high quantum yields, small particle size, and solution processability [8, 9]. A precise and efficient method for fabricating QD pixel arrays with dimensions less than 100 μm is needed to meet the industry demands for high-resolution, high-brightness, and high-efficiency displays [10]. Traditional approaches to fabricating QD color converters for micro-LED displays have faced several limitations. There are generally two ways to pattern color conversion material - printing processes and photolithography based methods.

Printing Methods

Inkjet printing (IJP) techniques have been employed to pattern QD films selectively. The QD films are deposited directly by piezoelectric nozzles in the print head, which ejects droplets of QD solution. The IJP methods are highly controllable, material efficient, and flexible; however, there are challenges in achieving small resolution, precise alignment, and uniform film thickness, which can impact display performance and yield [11, 12, 13, 14]. Electrohydrodynamic printing (EHDP) utilizes conductive nozzles and substrates as electrodes to generate an electric field that carefully guides the ink droplets to the desired locations [15]. EHDP can reduce the resolution limit of inkjet printing from 10 μm to less than 1 μm [16]. However, EHDP requires a conductive substrate, and the electric field may cause side effects on certain inks [17]. The thickness of printed films is usually limited [18]. Transfer printing methods involve assembling the QD material into an organized pattern on a master transfer substrate and then transferring the patterned layer to the final substrate [19, 20, 21]. The main benefits of transfer printing methods are their potential for achieving efficient mass transfer and scalability, but the requirement of a pre-structured master can reduce the flexibility of the process. Achieving high-accuracy alignment between the stamp and the final substrate is also challenging.

Photolithograhy-based Methods

Photolithography, a widely employed technique in the semiconductor industry, is not well-suited for patterning QD materials due to their sensitivity to the harsh chemicals involved

in the process. Direct photolithography using QD-filled photoresists has been explored, but the photoresist chemistry typically must be designed for specific QDs. Mixing the QD directly into photoresist often reduces efficiency, degrades optical properties, and can impose other limitations on the functionality of the film, though recent innovations with the photolithographic process have shown promise [22, 23, 24, 25, 26]. Qie et al. showed that QDs can be confined in a semiconductor polymer network frame to form high-quality patterns [27].

This thesis[1] presents a photolithography-based process for patterning solution-processed films utilizing a dry mechanical lift-off technique. The universal potential of this method is demonstrated through its compatibility with green perovskite quantum dots (QDs) and red CdSe/ZnS core-shell QDs. Additionally, the process is successfully executed at a wafer scale, achieving a high pattern resolution of approximately 1 μm and enabling multi-color patterning on the same substrate.

[1]**Nota bene:** This thesis is adapted from manuscript by Velpugonda J. L., Varnakavi N., Yerich M., Lin Y. L., titled "A Universal High-Resolution Micro-Patterning Technique for Solution-Processed Materials" submitted for publication in *Light: Advanced Manufacturing*

Chapter 2

METHODS

2.1 Dry Lift-Off Micro-Patterning Method

The principle of the dry lift-off micro-patterning process is illustrated in Figure 2.1. A clean substrate is coated with a buffer layer via chemical-vapor deposition (CVD). Currently, the process leverages the limited adhesion of parylene to various substrates and utilizes it as the buffer layer [28]. A typical photolithography is followed to show the pattern on the substrate. The pattern is then transferred onto the buffer layer using plasma etching. Subsequently, QDs are deposited on the substrate, and the buffer layer is mechanically peeled off, leaving behind the patterned QDs. In general, this method can pattern any solution-processed material and can be repeated for a full-color display. This method also allows for QD recycling by dissolving the peeled-off layer in QD solvent, which is an added benefit in a manufacturing process. Details of this method are further discussed in the Fabrication of Micro-Pattern section.

A wafer-scale processing of this method is necessary to validate its compatibility with standard semiconductor fabrication processes. In this study, a 4-inch glass wafer is used as the substrate and $CsPbBr_3$ perovskite QDs (PQDs) as the green color converter material, CdSe/ZnS core-shell QDs as red color converter material for the pattern. The PQDs were synthesized at room temperature using the ligand-assisted reprecipitation (LARP) method with triple-ligands [29, 30]. Although many methods for synthesizing PQDs exist, a room-temperature strategy is adopted due to its minimal requirements for environmental control factors such as temperature and inert gas conditions.

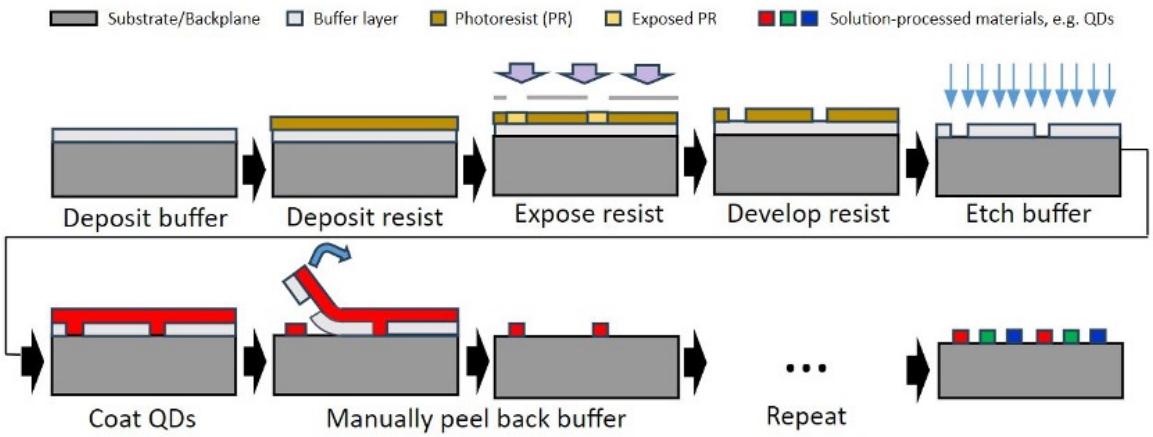

Figure 2.1: Diagram depicting the photolithography-based dry lift-off method for micro-patterning of multiple solution-processed films on a single substrate.

2.2 Perovskite QD Synthesis and Characterization

2.2.1 Materials

$PbBr_2$ (99.9 %), CsBr (99.9%), Cs_2CO_3 (99.9%), Octanoic acid (OTAc) ($\geq$ 99%), Didodecyldimethylammonium bromide (DDABr) (98%), Tetraoctylammonium bromide (TOABr) (98%) were purchased from Sigma-Aldrich. Toluene (99.8%, anhydrous) was purchased from ThermoFisher Scientific.

2.2.2 Synthesis

To synthesize green $CsPbBr_3$ PQDs, Cs_2CO_3 (0.5 mmol) was dissolved in 10 mL of OTAc to form the "Cs_2CO_3-in-OTAc solution." $PbBr_2$ (0.5 mmol) and 1 mmol of TOABr were added to 5 mL of toluene to create the "$PbBr_2$-and-TOAB solution." DDABr was dissolved in toluene at a concentration of 0.05 mol/L to prepare the "DDABr solution." Sequentially, 1 mL of the Cs2CO3-in-OTAc solution was injected into the $PbBr_2$-and-TOAB solution, followed by adding 1.3 mL of the DDAB solution. After 2 minutes, 11 mL of ethyl acetate was added. The resulting mixture was centrifuged at 10,000 rpm for 5 minutes, and the precipitates were dispersed in toluene. This centrifugation-redispersion cycle was repeated,

and the final PQDs precipitates were dispersed in toluene for further characterization.

2.2.3 Characterization

The morphology of the $CsPbBr_3$ PQDs was investigated using specific instrument models such as transmission electron microscopy (TEM) and high-resolution TEM (HR-TEM) images acquired on a FEI Tecnai G2 F20 S-TWIN HR(S)TEM operated at a 200 kV accelerating voltage. The $CsPbBr_3$ PQDs were drop-casted on a 300 mesh copper Formvar/carbon grid and dried in a vacuum overnight. Figure 2.2a shows the TEM image displaying square-shaped PQDs in a two-dimensional view. Based on symmetry, we can infer that the actual PQDs likely have a cubic-like shape in three dimensions. The bright regions between the dots are also distinct and continuous, suggesting a dense layer of surface ligands on the PQD surfaces. This dense coverage effectively prevents direct aggregation of the PQDs. The HRTEM image of a single PQD is shown in the upper-right inset of Figure 2.2a. It reveals a highly ordered crystalline lattice throughout the perovskite region. The measured interplanar distance between crystal planes is 0.58 nm, consistent with prior work [30]. The lower-right inset of Figure 2.2a is the particle size distribution histogram of the PQDs and reveals an average edge length of 11 $\pm$ 1.2 nm.

The PL spectra of perovskite films and patterns were measured by our home-made micro-PL system, which includes a continuous wave (CW) laser (λ = 405 nm) as the excitation source, an objective lens for focusing the laser beam onto the sample, a CCD camera(Chameleon 3, FLIR) for observing the laser beam location, and an optical spectrometer (OSM 100, Newport) for collecting the PL. The photoluminescence (PL) spectrum of the $CsPbBr_3$ PQD thin film exhibited a strong and narrow symmetric peak at 517 nm in the green region with a full-width half maximum of 19.5 nm, as shown in Figure 2.2b.

The PLQY of the PQD-dispersed toluene solutions was measured using an integrated sphere unit, with a CCD beam profiler (Thorlabs) for determining the focused beam size, and a silicon photodiode (Newport 818-UV) for measuring the power. The PLQY was calculated as the number of emitted photons divided by the number of absorbed photons. The $CsPbBr_3$ PQDs achieved a PL quantum yield (PLQY) of 93.6% (Figure 2.2c), indicating

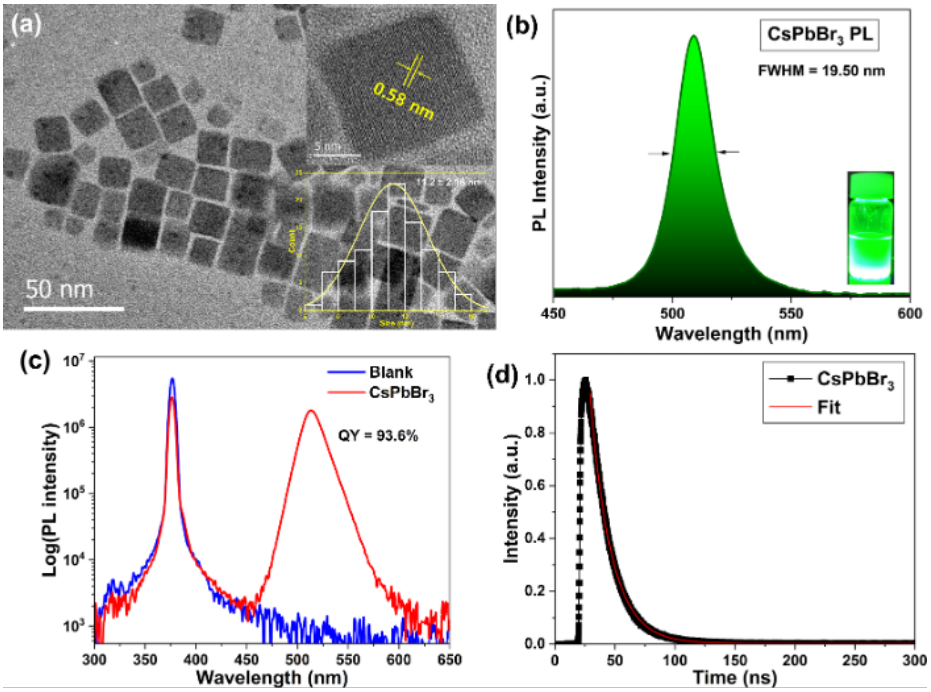

Figure 2.2: (a) TEM image of the $CsPbBr_3$ PQDs (inset image: corresponding HR-TEM and particle size distribution images), (b) PL spectrum of the PQD film (inset image: $CsPbBr_3$ PQDs in solution under UV light), (c) PLQY of the $CsPbBr_3$ PQDs in solution, and (d) TRPL decay curve of $CsPbBr_3$ PQDs.

that the triple-ligands effectively passivate the PQDs.

Time-resolved PL decays were measured using a time-correlated single photon counting system (FluoTime 100, PicoQuant) with a pulse laser excitation source (470 nm, 60 ps, 40 MHz). The TRPL curve shows exponential decay and is fitted to the bi-exponential decay function (Figure 2.2d), given in Eq. 1. The average lifetime was calculated using Eq. 2. [31, 32]

$y(t) = A_1 exp(-t/\tau_1) + A_2 exp(-t/tau_1)$, (Eq. 1)

$\tau_{ave} = (A_1\tau_1^2 + A_2\tau_2^2)/(A_1\tau_1 + A_2\tau_2)$, (Eq. 2)

Here, t represents time, A_1 and A_2 are weighing parameters which contribute to the decay components, τ_1 and τ_2 correspond to trap-assisted nonradiative recombination and free-charge carrier radiative recombination, respectively. After bi-exponential decay fitting, the estimated decay components τ_1 and τ_2 are 13.54 ns and 35.95 ns, respectively. The average decay time for $CsPbBr_3$ PQDs from the parameters obtained by the bi-exponential fit is 17.25 ns. The high PLQY and long lifetimes are attributed to the self-passivation effect due to the abundance of Br precursor during synthesis, which creates a high Br environment while suppressing surface defects. The synthesized $CsPbBr_3$ PQDs are utilized in the demonstration of single-color and multi-color displays.

2.3 CdSe/ZnS core-shell type QDs

The red CdSe/ZnS core-shell type QDs in toluene are purchased from Ocean NanoTech(QSR-620-50). These QDs have reported to have greater than 50% quantum yield from the vendor. The PL of these QDs is measured using ThorLabs compact CCD spectrometer(ccs100). The smoothed PL spectrum of the CdSe/ZnS QDs is shown in the Figure 2.3. The peak is measure to be around 620 nm.

2.4 Fabrication of Micro-Pattern using Dry Lift-Off Method

A 100mm glass wafer is chosen as the substrate to micro-pattern the QDs. The wafer undergoes initial cleaning through sonication in acetone and isopropanol (IPA) for 5 minutes each. Post-cleaning, the wafer is rinsed with deionized (DI) water and dried using a spin rinse dryer (SRD).

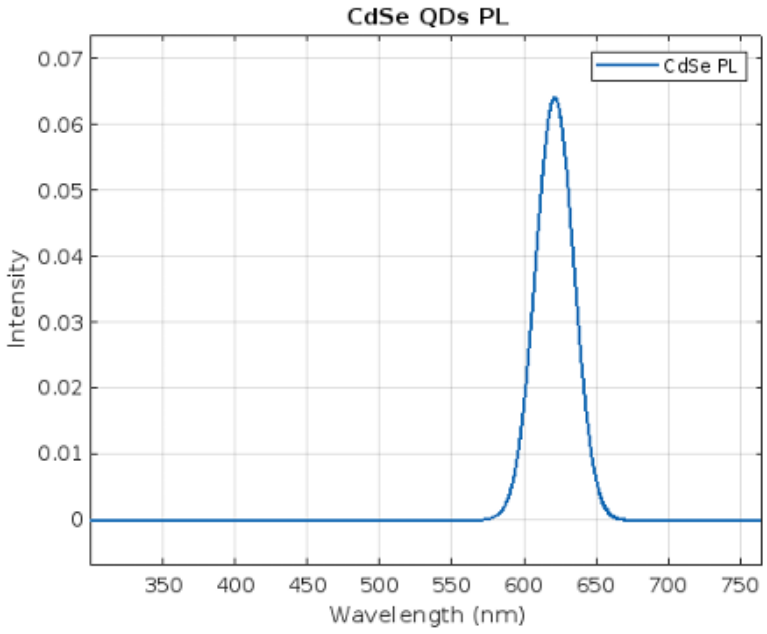

Figure 2.3: PL spectrum of CdSe/ZnS core-shell type QD film

2.4.1 Alignment layer

In order to align the different(green and red) QD layers on the substrate, alignment marks are first put down on the wafer using photolithography. An approximately 100 nm thick Al layer is deposited via sputter deposition (Evatec LLS EVO Sputter System), with 14 passes at a deposition rate of 7.4 nm/pass. The wafer is then spin-coated with AZ1512 positive photoresist in a two-step process: first, spinning at 500 rpm with an acceleration of 200 rpm/s for 5 seconds, followed by 4000 rpm at 1000 rpm/s for 60 seconds. The coated wafer is baked at 100°C for 120 seconds.

A UV exposure with a mercury arc lamp and an alignment mask is applied using an ABM SemiAuto Aligner, delivering a dosage of around 11.44 mJ/cm^2 at 400 nm for 9 seconds. The resist is developed in AD-10 developer for 70 seconds, rinsed with DI water, and dried using SRD. The developed photoresist mask facilitates etching of the Al layer, forming the alignment marks. The Al layer is etched using Aluminum Etch type A, which takes approximately 2 minutes. After etching, the wafer is rinsed in DI water and dried

using SRD. Finally, the resist mask is removed in an EKC bath for 5 minutes, followed by rinsing in a Cascade DI water bath for 3 minutes, and then dried using SRD.

2.4.2 Color conversion layer

A 6.3 g Parylene-C dimer is used to deposit a 3-μm-thick parylene layer via CVD (Specialty Coating Systems Model PDS2010 Labcoter). The furnace, vaporizer and vacuum setpoints are 690 °C, 175 °C and 35 mTorr, respectively. The deposition chamber was kept at room temperature. The parylene layer is then treated with O_2 plasma for better adhesion with the subsequently deposited Al layer. Plasma treatment is performed using Vision 320 RIE Mark II at 75 mTorr pressure and an O_2 flow rate of 100 sccm for 1 minute 30 seconds.

Following the dry lift-off micro-patterning process described earlier, the pattern is transferred to the parylene buffer layer using photolithography. Given the similar etch rates of parylene and photoresist, a thin 30 nm Al layer is used as a mask to etch parylene. This Al layer is deposited on the plasma-treated parylene layer via sputtering, with 4 passes at ≈7.4 nm/pass. Alignment marks are protected during sputtering with Al foil, which is removed post-deposition.

Using photolithography, the micro-pattern is transferred to the Al layer. The AZ1512 photoresist is spin-coated, baked, and exposed to UV under a manually aligned patterned mask following the alignment layer recipe. The substrate is developed in AD-10 developer for 75 seconds, rinsed with DI water in a cascade bath, and dried using SRD. The parylene is then etched using an Oxford ICP etcher at 10 mTorr pressure, 100 sccm O_2 flow rate, 75W RF power, and a temperature of 10°C for 5 minutes. Figures 3.1a, 3.2a show the substrate after the parylene etching.

Next, a QD(CdSe/ZnS) solution is drop-casted onto the substrate with a pipette and evenly dispersed. Once the QD film dries under a fume hood, the parylene layer is mechanically peeled off, leaving patterned QDs on the substrate.

2.4.3 Second color conversion layer

Before depositing the second color conversion layer, an SiO encapsulation layer is deposited on the patterned layer. This encapsulation protects the first color conversion layer during the subsequent patterning procedures. A 150 nm thick SiO layer is deposited using a PECVD tool (SPTS-SPM) at 125°C for 21 seconds at a deposition rate of 7.28 nm/sec. After encapsulation, the parylene layer is deposited and the same fabrication process is followed as previously described up to the QD deposition. The green $CsPbBr_3$ QD solution is then deposited, and once the film dries, the parylene layer is peeled off, leaving patterned green QDs on the substrate while protecting the underlying red QD layer.

Chapter 3

RESULTS AND DISCUSSION

3.1 Single-color Patterning

The process described in the section 2.4 was used to pattern the glass wafer with a mask featuring various pixel sizes ranging from 1 to 10 μm and pitch lengths of 22 μm and 9 μm. Figure 3.1a shows an optical microscope image of the wafer after the photoresist has been developed. The patterns are then transferred to the parylene layer, and PQDs are deposited by drop-casting. This method involves dispensing a solution containing PQDs onto the substrate, allowing it to spread and form a thin film. The buffer parylene layer is then mechanically peeled away, leaving the desired PQD patterned films on the wafer. This step is critical as it ensures that the PQDs are precisely patterned without any additional processing that could potentially alter their properties. Under a UV lamp, the bright green photoluminescence of the fabricated pixels is visible under a fluorescence microscope Figure 3.1b. The entire glass wafer, featuring various images patterned with green PQDs under UV illumination is shown in Figure 3.1c. The high-resolution images show the effectiveness of the dry lift-off process for patterning perovskites. The strong green luminescence and high color contrast observed in these patterns indicate the merits of this method in preserving the PQD optical quality and achieving clean patterns. The high resolution and uniformity of the patterns further highlight the precision of the technique.

To demonstrate the universal applicability of this method, the red CdSe/ZnS QDs discussed in section 2.3 were patterned on the substrate. As with the green PQDs, the red QDs are patterned via the dry mechanical lift-off method. Following the deposition of red CdSe/ZnS QDs, the parylene layer is mechanically peeled off, revealing the desired pattern on the wafer Figure 3.2a-c. The bright red luminescence and clear pattern confirmed the successful dry lift-off process application for these QDs. The high color contrast and strong luminescence indicate that the QDs maintain their optical quality and performance after

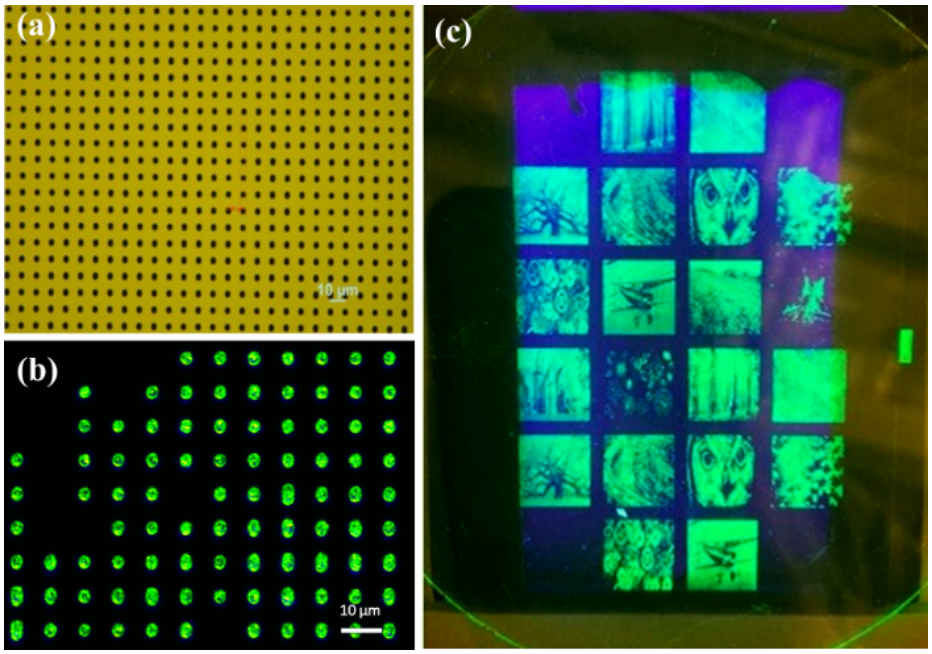

Figure 3.1: (a) Optical microscope image of the photoresist layer after developing, (b) fluorescence microscope image of micro-patterned green PQD pixels, and (c) glass wafer displaying different images patterned with green PQDs under a UV lamp.

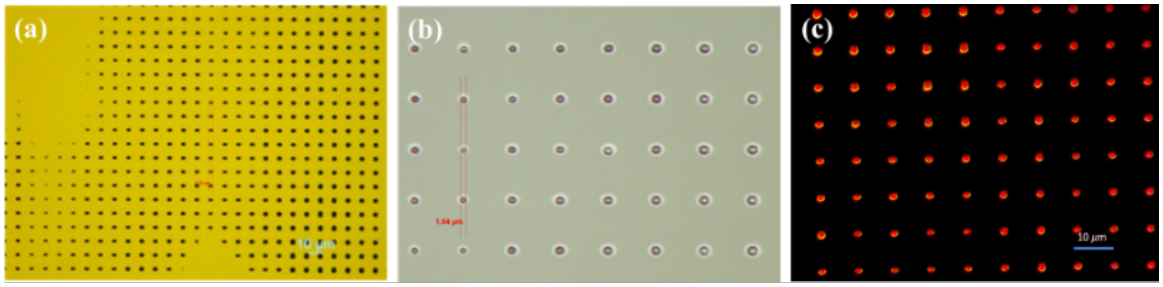

Figure 3.2: (a) Wafer after the pattern is developed on the substrate, (b) optical microscope image of red CdSe/ZnS QDs patterned on the glass wafer showing feature size of 1.04 µm, and (c) fluorescence microscope image of red CdSe/ZnS QDs.

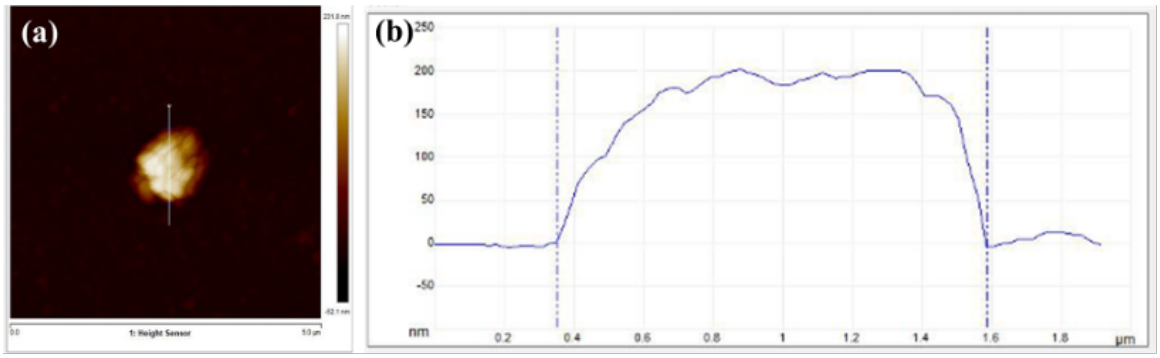

Figure 3.3: a) 2D height profile from AFM of a single patterned QD feature, and (b) cross-sectional height profile of the QD feature showing a diameter of 1.2 µm and height of 180 nm. The profile is taken along the vertical arrow in (a).

patterning.

Figure 3.3a displays a detailed two-dimensional height profile of a 5 × 5 µm sample area, obtained using atomic force microscopy (AFM). This technique offers high-resolution imaging of the sample's surface topography, enabling precise measurement of surface features. Additionally, a cross-sectional height profile scanned along the vertical axis of this area is shown in Figure 3.3b. This cross-sectional view highlights height variations across the sample, which are crucial for evaluating the uniformity and thickness of the pattern. These measurements show the QD color converter has an approximate width and height of 1.2 μm and 180 nm, respectively.

3.2 Multi-color Patterning

To achieve a full-color display, it is desirable to pattern green, red, and sometimes blue color converter pixels on a single substrate with a blue or UV backlight underneath. The blue or UV light is absorbed by the QD pixels, which re-emit green, red or blue light via photoluminescence [33, 34, 35]. Following the described fabrication steps in section 2.4 green PQDs and red CdSe/ZnS QDs were successfully patterned on the same substrate. The red QDs were patterned first on the wafer and SiO encapulating layer was subsequently followed. Next, a new parylene layer was deposited on top of the patterned red QDs. The same photolithography and etching processes were then applied to the new parylene layer to create the pattern for the green PQDs. The green PQDs were deposited onto the substrate, and the parylene layer was peeled off, revealing the green QD pattern integrated with the previously patterned red QDs. The wafer now features red and green QDs patterned on the same substrate, demonstrating the two-color patterning capability of this method. Figure 3.4 depicts fluorescence microscope images of the patterned two-color arrays. The smallest feature sizes achieved were approximately 2 µm, indicating the high resolution and precision of the patterning process. This successful demonstration of multi-color patterning underscores the versatility and effectiveness of the dry lift-off method for creating complex, high-resolution patterns with QDs of vastly different types.

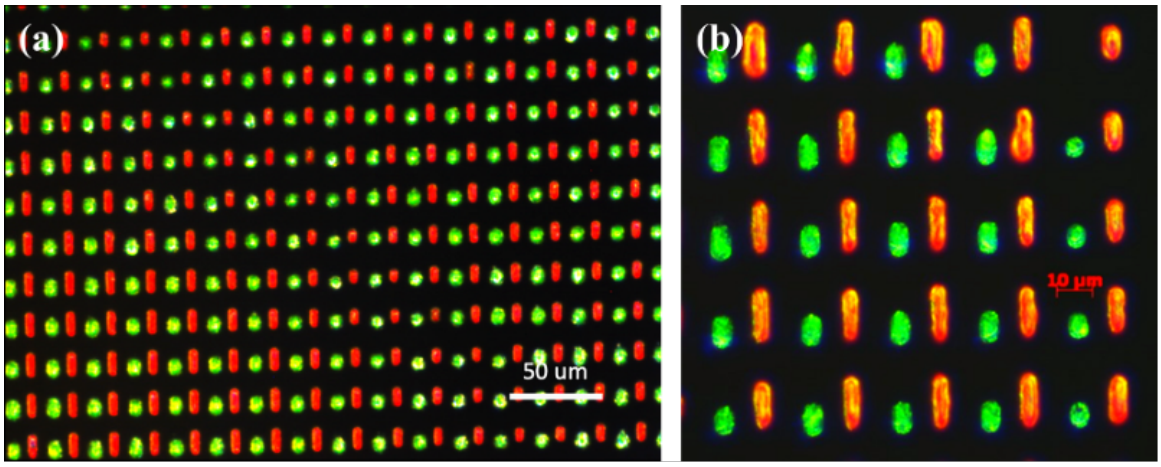

Figure 3.4: a) Fluorescence microscope image of multi-color patterns integrating green perovskite QDs and red CdSe/ZnS QDs using the dry lift-off method, and (b) enlarged image of the multi-color pattern.

Chapter 4

CONCLUSION AND PROSPECTS

The reported results demonstrate a high-resolution, large-area photolithographic approach for patterning QD color converter thin films with parylene as an intermediate. Parylene is used to facilitate a dry lift-off procedure, in which undesired QDs are mechanically removed without the use of additional solvents. A pattern resolution close to 1 µm is achieved.

Since the QDs are deposited as the final step and do not undergo any further processing, their PL properties and narrow linewidth are preserved. This ensures that the QDs retain high performance and optical quality, making this technique highly attractive for applications requiring precise and reliable patterning of solution-processed materials. Additionally, preserving the optical properties of QDs is crucial for their use in optoelectronic devices, where consistent performance and efficiency are essential.

This method has been used successfully to create single-color and multi-color patterns. The parylene coatings effectively shield the underlying QD films, allowing for the creation of multi-color color converter patterns through repeated use of the usual photolithography technique. Furthermore, since the method is agnostic to the materials to be patterned, QDs of different types can be integrated, which was demonstrated by the successful integration of green PQDs with red CdSe/ZnS QDs. The display industry has not come to a consensus on the optimum QDs. InP QDs are appealing for being non-toxic, and their optical quality has been improving [36]. The universality of the dry lift-off micro-patterning method can ensure agile adaptation to any adopted materials.

These results demonstrate the versatility of the method to micro-pattern solution-processed materials with high resolution. The simplicity and effectiveness of this method also make it a promising approach for large-scale manufacturing and integration of QD-based devices, potentially lowering production costs and increasing accessibility for various applications.

Future Work Outlook

This work has demonstrated a multi-color display using Quantum Dots (QDs) as color conversion materials, presenting a prototype that displays a static image with a UV backlight source. Moving forward, the next step involves developing a full-color display by integrating blue or UV pixel sources. This advancement would enable this technology to compete with the current display industry.

In addition to enhancing color conversion technology, pursuing self-emissive display technology offers several advantages, including superior contrast, faster response times, improved energy efficiency, and slimmer designs. Among solution-based emitters, perovskites have emerged as leading candidates due to their narrow emission bandwidth and high efficiency. Notably, a green pixelated perovskite micro-LED array has been demonstrated by Chen et al. using the dry lift-off method [28]. Despite these advancements, progress in developing blue perovskite LEDs (PeLEDs) has lagged behind that of red and green counterparts. Furthermore, there is a need to enhance the operational stability of PeLEDs to meet the demands of practical applications. Addressing these challenges will be crucial for advancing the technology.

Another objective for the dry lift-off method in the display technology is to achieve a self-emissive, full-color micro-LED display integrated with a thin-film transistor (TFT) backplane. Future research should focus on the integration of RGB (red, green, and blue) PeLEDs(or solution based emitters) on a single substrate to realize this goal. Achieving this would not only mark a significant milestone in display technology but also pave the way for more efficient, cost-effective displays with broad application potential.

BIBLIOGRAPHY

[1] H. Y. Hsiang En-Lin, Deng Ming-Yang, "Mini-led, micro-led and oled displays: present status and future perspectives," *Light Sci Appl*, vol. 9, p. 105, June 2020.

[2] T.-Y. Lee, L.-Y. Chen, Y.-Y. Lo, S. S. Swayamprabha, A. Kumar, Y.-M. Huang, S.-C. Chen, H.-W. Zan, F.-C. Chen, R.-H. Horng, and H.-C. Kuo, "Technology and applications of micro-leds: Their characteristics, fabrication, advancement, and challenges," *ACS Photonics*, vol. 9, no. 9, pp. 2905–2930, 2022.

[3] V. W. Lee, N. Twu, and I. Kymissis, "Micro-led technologies and applications," *Information Display*, vol. 32, no. 6, pp. 16–23, 2016.

[4] R. S. Cok, M. Meitl, R. Rotzoll, G. Melnik, A. Fecioru, A. J. Trindade, B. Raymond, S. Bonafede, D. Gomez, T. Moore, C. Prevatte, E. Radauscher, S. Goodwin, P. Hines, and C. A. Bower, "Inorganic light-emitting diode displays using micro-transfer printing," *Journal of the Society for Information Display*, vol. 25, no. 10, pp. 589–609, 2017.

[5] D. Lee, S. Cho, C. Park, K. R. Park, J. Lee, J. Nam, K. Ahn, C. Park, K. Jeon, H. Yuh, W. Choi, C. H. Lim, T. Kwon, Y. H. Min, M. Joo, Y.-H. Choi, J. S. Lee, C. Kim, and S. Kwon, "Fluidic self-assembly for MicroLED displays by controlled viscosity," *Nature*, vol. 619, pp. 755–760, July 2023.

[6] C. Yan, G. Liang, G. Liu, Y. Tang, J. Li, and Z.-T. Li, "Eliminating the residual ultraviolet excitation light and increasing quantum dot emission intensity in led display devices," *IEEE Transactions on Electron Devices*, vol. 68, no. 2, pp. 584–591, 2021.

[7] Y. H. Kim, N. S. M. Viswanath, S. Unithrattil, H. J. Kim, and W. B. Im, "Review—phosphor plates for high-power led applications: Challenges and opportunities toward perfect lighting," *ECS Journal of Solid State Science and Technology*, vol. 7, p. R3134, oct 2017.

[8] Y. E. Panfil, M. Oded, and U. Banin, "Colloidal quantum nanostructures: Emerging materials for display applications," *Angewandte Chemie International Edition*, vol. 57, no. 16, pp. 4274–4295, 2018.

[9] F. P. G. de Arquer, D. V. Talapin, V. I. Klimov, Y. Arakawa, M. Bayer, and E. H. Sargent, "Semiconductor quantum dots: Technological progress and future challenges," *Science*, vol. 373, no. 6555, p. eaaz8541, 2021.

[10] J. Chen, Q. Zhao, B. Yu, and U. Lemmer, "A review on quantum dot-based color conversion layers for mini/micro-led displays: Packaging, light management, and pixelation," *Advanced Optical Materials*, vol. 12, no. 2, p. 2300873, 2024.

[11] L. Shi, L. Meng, F. Jiang, Y. Ge, F. Li, X.-g. Wu, and H. Zhong, "In situ inkjet printing strategy for fabricating perovskite quantum dot patterns," *Advanced Functional Materials*, vol. 29, no. 37, p. 1903648, 2019.

[12] J. Lemarchand, N. Bridonneau, N. Battaglini, F. Carn, G. Mattana, B. Piro, S. Zrig, and V. Noël, "Challenges, prospects, and emerging applications of inkjet-printed electronics: A chemist's point of view," *Angewandte Chemie International Edition*, vol. 61, no. 20, p. e202200166, 2022.

[13] C.-T. Lin, Y.-l. Zhuan, N.-T. Jung, M.-S. Hoang, and H.-S. Chen, "Design of quantum dot color convertors for inkjet-printed optoelectronic devices: Violet-converted full color mini-led," *Advanced Materials Technologies*, vol. 9, no. 3, p. 2301370, 2024.

[14] T. Xuan, S. Shi, L. Wang, H.-C. Kuo, and R.-J. Xie, "Inkjet-printed quantum dot color conversion films for high-resolution and full-color micro light-emitting diode displays," *The Journal of Physical Chemistry Letters*, vol. 11, no. 13, pp. 5184–5191, 2020. PMID: 32531168.

[15] M. S. Onses, E. Sutanto, P. M. Ferreira, A. G. Alleyne, and J. A. Rogers, "Mechanisms, capabilities, and applications of high-resolution electrohydrodynamic jet printing," *Small*, vol. 11, no. 34, pp. 4237–4266, 2015.

[16] H. Li, Y. Duan, Z. Shao, G. Zhang, H. Li, Y. Huang, and Z. Yin, "High-resolution pixelated light emitting diodes based on electrohydrodynamic printing and coffee-ring-free quantum dot film," *Advanced Materials Technologies*, vol. 5, no. 10, p. 2000401, 2020.

[17] X. Yang, S. Wang, Y. Hou, Y. Wang, T. Zhang, Y. Chen, G. Chen, C. Zhong, X. Fan, X. Kong, T. Wu, Y. Lu, Y. Lin, and Z. Chen, "Dual-ligand red perovskite ink for electrohydrodynamic printing color conversion arrays over 2540 dpi in near-eye micro-led display," *Nano Letters*, vol. 24, no. 12, pp. 3661–3669, 2024. PMID: 38408021.

[18] Y. Liang, J. Yong, Y. Yu, A. Nirmalathas, K. Ganesan, R. Evans, B. Nasr, and E. Skafidas, "Direct electrohydrodynamic patterning of high-performance all metal oxide thin-film electronics," *ACS Nano*, vol. 13, no. 12, pp. 13957–13964, 2019. PMID: 31793762.

[19] T. Meng, Y. Zheng, D. Zhao, H. Hu, Y. Zhu, Z. Xu, S. Ju, J. Jing, X. Chen, H. Gao, K. Yang, T. Guo, F. Li, J. Fan, and L. Qian, "Ultrahigh-resolution quantum-dot light-emitting diodes," *Nature Photonics*, vol. 16, pp. 297–303, Apr. 2022.

[20] J. I. Kwon, G. Park, G. H. Lee, J. H. Jang, N. J. Sung, S. Y. Kim, J. Yoo, K. Lee, H. Ma, M. Karl, T. J. Shin, M. H. Song, J. Yang, and M. K. Choi, "Ultrahigh-resolution full-color perovskite nanocrystal patterning for ultrathin skin-attachable displays," *Science Advances*, vol. 8, no. 43, p. eadd0697, 2022.

[21] J. Bae, Y. Shin, H. Yoo, Y. Choi, J. Lim, D. Jeon, I. Kim, M. Han, and S. Lee, "Quantum dot-integrated GaN light-emitting diodes with resolution beyond the retinal limit," *Nature Communications*, vol. 13, p. 1862, Apr. 2022.

[22] C.-C. Lin, K.-L. Liang, H.-Y. Chao, C.-I. Wu, S. f. Lin, B.-M. Huang, C.-W. Huang, C.-C. Wu, W.-H. Kuo, and Y.-H. Fang, "Fabricating quantum dot color conversion layers for micro-led-based augmented reality displays," *ACS Applied Optical Materials*, vol. 2, no. 7, pp. 1303–1313, 2024.

[23] P. Zhang, G. Yang, F. Li, J. Shi, and H. Zhong, "Direct in situ photolithography of perovskite quantum dots based on photocatalysis of lead bromide complexes," *Nature Communications*, vol. 13, p. 6713, Nov. 2022.

[24] D. Liu, K. Weng, S. Lu, F. Li, H. Abudukeremu, L. Zhang, Y. Yang, J. Hou, H. Qiu, Z. Fu, X. Luo, L. Duan, Y. Zhang, H. Zhang, and J. Li, "Direct optical patterning of perovskite nanocrystals with ligand cross-linkers," *Science Advances*, vol. 8, no. 11, p. eabm8433, 2022.

[25] J.-A. Pan, J. C. Ondry, and D. V. Talapin, "Direct optical lithography of cspbx3 nanocrystals via photoinduced ligand cleavage with postpatterning chemical modification and electronic coupling," *Nano Letters*, vol. 21, no. 18, pp. 7609–7616, 2021. PMID: 34478618.

[26] D. Hahm, J. Lim, H. Kim, J.-W. Shin, S. Hwang, S. Rhee, J. H. Chang, J. Yang, C. H. Lim, H. Jo, B. Choi, N. S. Cho, Y.-S. Park, D. C. Lee, E. Hwang, S. Chung, C.-M. Kang, M. S. Kang, and W. K. Bae, "Direct patterning of colloidal quantum dots with adaptable dual-ligand surface," *Nature Nanotechnology*, vol. 17, pp. 952–958, Sept. 2022.

[27] Y. Qie, H. Hu, K. Yu, C. Zhong, S. Ju, Y. Liu, T. Guo, and F. Li, "Ligand-nondestructive direct photolithography assisted by semiconductor polymer cross-linking for high-resolution quantum dot light-emitting diodes," *Nano Letters*, vol. 24, no. 4, pp. 1254–1260, 2024. PMID: 38230959.

[28] C. Zou, C. Chang, D. Sun, K. F. Böhringer, and L. Y. Lin, "Photolithographic patterning of perovskite thin films for multicolor display applications," *Nano Letters*, vol. 20, no. 5, pp. 3710–3717, 2020. PMID: 32324409.

[29] Y. Liu, S. Tang, J. Fan, E. Gracia-Espino, J. Yang, X. Liu, S. Kera, M. Fahlman, C. Larsen, T. Wågberg, L. Edman, and J. Wang, "Highly soluble cspbbr3 perovskite quantum dots for solution-processed light-emission devices," *ACS Applied Nano Materials*, vol. 4, no. 2, pp. 1162–1174, 2021.

[30] J. Song, J. Li, L. Xu, J. Li, F. Zhang, B. Han, Q. Shan, and H. Zeng, "Room-temperature triple-ligand surface engineering synergistically boosts ink stability, recombination dynamics, and charge injection toward eqe-11.6% perovskite qleds," *Advanced Materials*, vol. 30, no. 30, p. 1800764, 2018.

[31] Q. Mo, T. Shi, W. Cai, S. Zhao, D. Yan, J. Du, and Z. Zang, "Room temperature synthesis of stable silica-coated cspbbr3 quantum dots for amplified spontaneous emission," *Photon. Res.*, vol. 8, pp. 1605–1612, Oct 2020.

[32] S. Kachhap, S. Fatima, A. Yadav, A. K. Singh, and S. K. Singh, "Expanding the emission of cspbbr3 nanocrystals in the blue region," *ACS Applied Optical Materials*, vol. 1, no. 12, pp. 1974–1986, 2023.

[33] X. Dai, Y. Deng, X. Peng, and Y. Jin, "Quantum-dot light-emitting diodes for large-area displays: Towards the dawn of commercialization," *Advanced Materials*, vol. 29, no. 14, p. 1607022, 2017.

[34] S. Lin, G. Tan, J. Yu, E. Chen, Y. Weng, X. Zhou, S. Xu, Y. Ye, Q. F. Yan, and T. Guo, "Multi-primary-color quantum-dot down-converting films for display applications," *Opt. Express*, vol. 27, pp. 28480–28493, Sep 2019.

[35] Y. Wu, J. Ma, P. Su, L. Zhang, and B. Xia, "Full-color realization of micro-led displays," *Nanomaterials*, vol. 10, no. 12, 2020.

[36] B. Karadza, P. Schiettecatte, H. Van Avermaet, L. Mingabudinova, L. Giordano, D. Respekta, Y.-H. Deng, I. Nakonechnyi, K. De Nolf, W. Walravens, Y. Meuret, and Z. Hens, "Bridging the green gap: Monochromatic inp-based quantum-dot-on-chip leds with over 50% color conversion efficiency," *Nano Letters*, vol. 23, no. 12, pp. 5490–5496, 2023. PMID: 37310759.